Contrib. Astron. Obs. Skalnaté Pleso **55/2**, 69 – 80, (2025)
https://doi.org/10.31577/caosp.2025.55.2.69

Stark broadening parameters for 6s ^{4}F - 6p ^{4}(D, F, G)^o supermultiplet of singly ionized Hafnium

Z. Simić[1], M.S. Dimitrijević[1,2] and N. Sakan[3]

[1] *Astronomical Observatory, Volgina 7, 11060 Belgrade, Serbia (E-mail: zsimic@aob.rs)*

[2] *LERMA, Observatoire de Paris, F-92195 Meudon Cedex, France*

[3] *University of Belgrade, Institute of Physics, PO Box 57, 11001 Belgrade, Serbia*

Received: November 19, 2024; Accepted: December 03, 2024

Abstract. Stark broadening parameters - line widths and shifts - are of interest in stellar spectroscopy as well as in laboratory and technological plasmas. Stark widths and shifts have been calculated for 28 Hf II transitions using plasma electron density of 10^{17}cm^{-3} and temperature from 5000K to 80000K as parameters. The calculations were performed according to the simplified modified semiempirical (SMSE) method.

Key words: Stark broadening – line profiles – atomic data

1. Introduction

Insight into impact broadening parameters is of great importance for stellar spectroscopy and laboratory and technological plasma. In this context, stellar abundances must be both precise and accurate in order to obtain reliable information about the stellar atmospheres chemical composition. For example, in metal-poor stars, the strongest and often the only discernible lines of heavy elements are found in ultraviolet (UV) range, from 1000 to 4000 Å and visible blue from 4400 to 4900 Å, Roederer et al. (2012). Absorption lines of interest in these parts of the spectrum are likely to be blended with lines from other sources. To obtain accurate abundances, valid atomic data are necessary, and the electronic level populations in the line-forming layers of the atmosphere must be reliably modeled.

The first determination of the amount of solar hafnium was performed by Russell (1929). The value of A(Hf)=0.90 was surprisingly accurate for the time. In Andersen et al. (1976), the abundance of solar hafnium was redetermined, and reliable transition probabilities for Hf II were obtained. Photospheric spectra were obtained using the McMath Solar Telescope at Kitt Peak National Observatory, Arizona, USA. These analysis was carried out by means of the method of spectrum synthesis. Lifetime measurements of nine Hf II levels have been performed by the beam-foil technique. These dominant spectral lines of Hf II in the solar spectrum and their upper levels were selected for this investigation. All Hf II lines investigated are situated in regions where numerous absorption lines occur.

The first detection of Hf II in a metal-poor halo star was reported in Sneden et al. (1996) in the spectrum of CS 22892-052 (two Hf II lines at 3719.28 Å and 3793.38 Å), with a mean abundance of log ϵ=-0.90±0.10. They compared their results with calculated contributions of r- and s-processes in the solar abundances, scaling the solar pattern to best fit the abundances of the $56\leq Z\leq 76$ elements. Elemental abundance in CS 22892-052 was reanalyzed by Sneden et al. (2003) who obtained the new value of log ϵ=-0.98±0.10.

In Den Hartog et al. (2021), authors recorded blue and UV spectra of several metal-poor stars and noticed many lines of singly ionized hafnium. Their report noted new measurements of the branching fraction for 199 UV and optical transitions of Hf II. These transitions range in wavelength (wavenumber) from 2068 to 6584 Å. With these these new transition probabilities it was derived and improved Hf abundances in two metal-poor stars. These lines show potential to be useful abundance indicators, for the stars namely HD 196944 enhanced in s-process elements and HD 222925 enhanced in r-process elements.

Hafnium is very important for nucleosynthesis of heavy elements. Improved laboratory data, especially atomic transition probabilities, are essential for using Hf as a reference element. New results were reported in Lawler et al. (2007), indicating Hf as a suitable stable reference element for nucleocosmochronometry, where it can serve for improved stellar age determination.

In Lawler et al. (2007), authors also disclosed radiative lifetimes of 8 Hf I and 18 Hf II levels, measured with the laser induced fluorescence technique. Branching fractions for transitions from the Hf II levels have been measured from the Fourier transform spectra. Combining the new lifetimes with the Branching fractions, 195 absolute oscillator strengths have been derived. In addition to the Branching fractions, accurate wavelengths for the 195 Hf II lines were measured. These data were applied in the determination of hafnium abundance in the chemically peculiar stars χ Lupi (HgMn) and HR 3383 (hot-Am), and were discussed in terms of possible revisions of the hafnium abundance for the Sun and the galactic halo stars CS 22892-052 and CS 31082-001 (see references Hill et al. (2002); Yushchenko et al. (2005); Ivarsson et al. (2003) for details).

2. Method

We used the simplified modified semiempirical method Dimitrijević & Konjević (1987), designed for Stark broadening of isolated spectral lines of singly and multiply charged ions in plasma. A more accurate semiclassical perturbation method Sahal-Bréchot (1969a,b); Sahal-Brechot et al. (2014) is not applicable in an adequate way due to insufficient atomic data. Precise information on the closest perturber levels for both initial and final states of the transition is crucial for impact broadening parameters calculation.

Accordingly, full width at half maximum intensity reads:

$$w_{smse}=K_{fw}\frac{\lambda^2 N}{\sqrt{T}}(0.9-\frac{1.1}{Z})\sum_{k=i,f}\left(\frac{3n^*_{l_k}}{2Z}\right)^2({n^*_{l_k}}^2-{l_k}^2-l_k-1) \tag{1}$$

where λ[m] is the wavelength, N[m^{-3}] denotes the perturber density, T[K] the temperature, $K_{fw}=2.21577\cdot10^{-20}$ m^{2}K$^{1/2}$ is a constant and w_{smse}[m] is the full width at half maximum intensity. Initial atomic energy level is denoted by i and the final with f $(k=i,f)$. Z denotes ion residual charges: $Z=1$ for neutral, $Z=2$ for singly ionized, $Z=3$ for doubly ionized, etc. Effective principal quantum number is labeled $n^*_{l_k}$, where l_k $(k=i,f)$ represents orbital angular momentum quantum number.

Formula for the Stark shift calculation depends on whether the transitions with $\Delta n=0$ (where n denotes the main principal number) when all transition for $l+1$ and $l-1$ exist or not, as for example for s energy levels, where transition with $l-1$ is missing. Its general form reads:

$$d_{smse}\approx K_{sh}\frac{\lambda^2 N}{\sqrt{T}}(0.9-\frac{1.1}{Z})\frac{9}{4Z^2}S \tag{2}$$

where K_{sh}=1.1076$\cdot10^{-20}$ m^{2}K$^{1/2}$ is a constant and the polynomial S is calculated either like:

$$S_1=\sum_{k=i,f}\frac{{n^*_{l_k}}^2\epsilon_k}{2l_k+1}({n^*_{l_k}}^2-3{l_k}^2-3l_k-1) \tag{3}$$

if all transition with $l+1$ and $l-1$ exist, or according to:

$$S_2=\sum_{k=i,f}\frac{{n^*_{l_k}}^2\epsilon_k}{2l_k+1}[(l_k+1)[{n^*_{l_k}}^2-(l_k+1)^2]-l_k({n^*_{l_k}}^2-l_k^2)] \tag{4}$$

in general; $\epsilon_k=+1$ for $k=i$ and $\epsilon_k=-1$ for $k=f$.

We used the following expression to calculate the averaged energies:

$$E=\frac{\sum_J(2J+1)E_J}{\sum_J(2J+1)} \tag{5}$$

where E represents the averaged energy in units cm^{-1}, E_J energy level and J the total angular momentum of a particular level.

3. Results and discussion

In this contribution, the research was continued on the singly ionized element Hafnium, which expands the list of the heavier elements that we tackled in the previous studies: iridium Simić et al. (2021), rhodium Simić & Sakan (2021) and rhenium Simić et al. (2023). The Stark broadening parameters were obtained - the widths and shifts of 28 Hf II spectral lines, according to the simplified modified semi-empirical method.

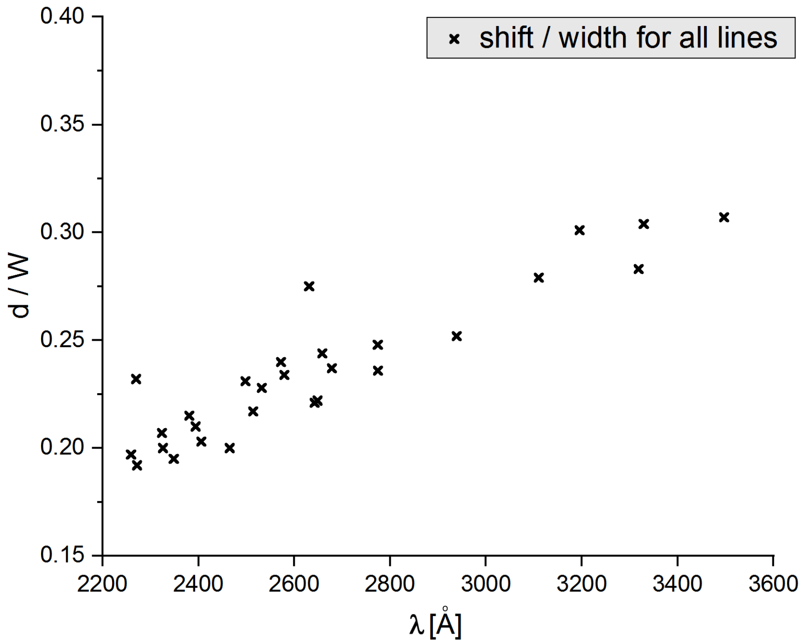

Figure 1. Ratio of calculated Stark shifts and widths for all spectral lines of singly ionized hafnium.

All calculations were performed using the electron density of 10^{17}cm^{-3} and temperatures from 5000 to 80000 K. Energy levels were taken from Moore (1971). Our results for the Hf II spectral lines are presented in Table 1. The first column presents transitions with calculated wavelengths, which may differ from the experimental ones. The second one contains the predefined temperatures, and the next two pairs of columns give the corresponding data for Stark width and shift in Å, as well as in angular frequency units. The latter are calculated according to the formulas:

$$W[\mathrm{s}^{-1}] = \frac{2\pi c}{\lambda^2} W \tag{6}$$

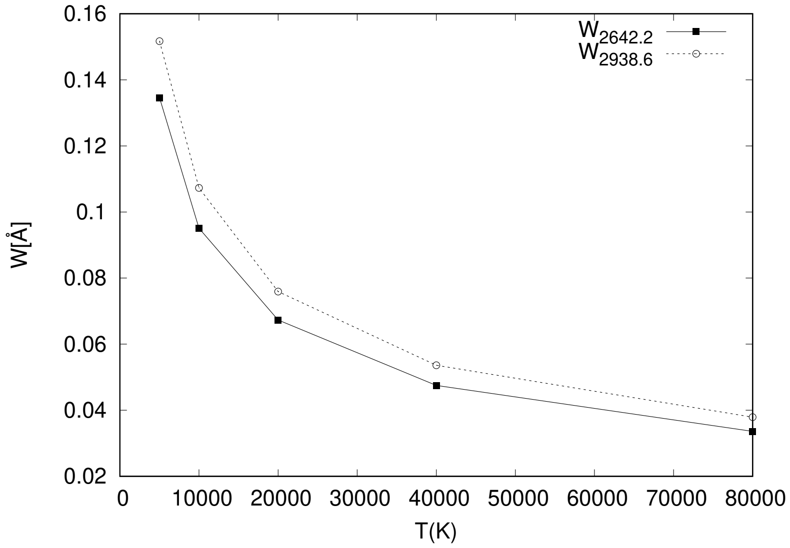

Figure 2. Dependence of width on temperature for 2642.2 Å and 2938.6 Å spectral lines of singly ionized hafnium of multiplet 6s ^{4}F - 6p ^{4}G^O.

$$d[\mathrm{s}^{-1}] = \frac{2\pi c}{\lambda^2} d \tag{7}$$

where c is the light speed in inits m/s. The last column gives $3\mathrm{k}T/2\Delta E$, where ΔE is the energy difference between the nearest perturbing level and the closest of the starting and ending levels. The $3\mathrm{k}T/2\Delta E$ term must be less than or equal to two for the method to be valid. To determine the width or shift for an arbitrary experimental wavelength λ_{exp}, the following expressions should be used:

$$W_{exp} = (\frac{\lambda_{exp}}{\lambda})^2 W \tag{8}$$

$$d_{exp} = (\frac{\lambda_{exp}}{\lambda})^2 d \tag{9}$$

where W_{exp} and d_{exp} are the width and shift for an experimental λ_{exp}, and λ is a theoretical wavelength, with corresponding W and d (the width and shift) in Table 1.

In our calculations, we considered the supermultiplet of singly ionized hafnium 5d^2(a^{3}F)6s ^{4}F - 5d^2(a^{3}F)6p ^{4}(D, F, G)^O, which consists of the following multiplets with the identical parent term 5d^2(a^{3}F) for both the initial and final level. The first one is 6s ^{4}F - 6p ^{4}D^O with 9 spectral lines, the second one is 6s ^{4}F - 6p ^{4}F^O with 10 spectral lines and the third one is 6s ^{4}F - 6p ^{4}G^O with

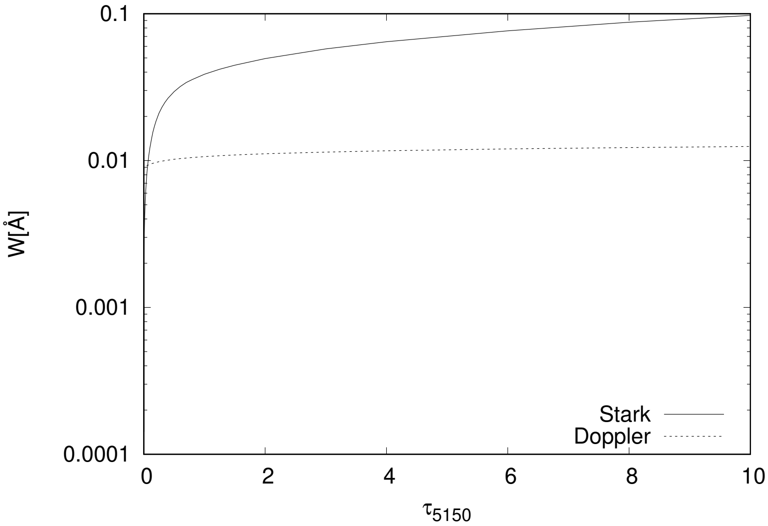

Figure 3. Thermal Doppler and Stark widths for Hf II 2642.2 Å spectral line of singly ionized hafnium of multiplet 6s ^{4}F - 6p ^{4}G^O for DA white dwarf atmosphere model with T_{eff} = 15000 K and log $g = 8$, as a function of optical depth τ_{5150}.

9 spectral lines, all of which fulfill the conditions of LS-coupling or Russell-Saunders coupling for connection and the selection rules. All labels are taken from Moore (1971); Reader et al. (1980); Ralchenko et al. (2005) and the NIST database, at site https://www.nist.gov/.

Taking into account the entire set of calculated spectral lines of singly ionized hafnium, we compared the shift and line width ratios (d/W) for each one, which can be seen in Figure 1. This ratio does not depend on the wavelength, temperature or density of the perturber, but it does depend on the quantum numbers and the optical charge seen by the electron. Minimum value of the ratio of 0.197 occurs for the 2259.4 Å line. The ratio increases approximately linearly with the wavelength, up to value 0.307 for the highest wavelength of 3496.8 Å.

For some of the calculated lines of singly ionized hafnium there are relative intensity presented in the NIST database. One of them has relative intensity of 1100 and it is observed at 2642.2 Å, which belongs to the multiplet 6s a^{4}F$_{9/2}$ - 6p z^{4}G$^o_{11/2}$, as well as the second strongest line of 2938.6 Å, with the relative intensity of 710. The Figure 2 shows the dependence of width on temperature, we notice that as the temperature increases, the width of the line decreases faster - the interval below 40000 K, and more slowly at higher temperatures than this. The spectral line 6s a^{4}F$_{9/2}$ - 6p z^{4}G$^o_{9/2}$ with wavelenght is 2938.6 Å from multiplet 6s ^{4}F - 6p ^{4}G^O was compared with the 2642.2 Å line. This results is in accordance with the Eq. (1), given in the previous section, which provides dependencies from the wavelength and the initial and final energy levels.

In order to determine the influence of the Stark broadening in the atmosphere of hot stars, especially white dwarfs and check its importance and contribution, we tested the spectral line on the DA type model Wickramasinghe (1972) of white dwarfs, with T_{eff} = 15000 K and log g = 8. Here, we denoted with τ_{5150} optical depth points at the standard wavelength λ_s=5150 Å also used in Wickramasinghe (1972). As can be seen from Figure 3 Stark broadening mechanism is more dominant in comparison with thermal Doppler, starting from the lowest photosphere layer in the atmosphere of the white dwarf. Our result shows 2642.2 Å spectral line from the multiplet 6s ^{4}F - 6p ^{4}G^O.

Insight into Stark broadening parameters is of great importance for the interpretation of spectra of A-type stars and white dwarfs, as we have shown in some of the previous studies Majlinger et al. (2015, 2017); Simić & Sakan (2020); Simić & Sakan (2021). Therefore, the Stark broadening must be taken into consideration when investigating stellar, technological and laboratory plasma.

4. Conclusion

In this paper, the selected transition metal is singly charged hafnium ion, which is detected in atmospheres of metallic stars, as for examle the spectrum of CS 22892-052. This element whose energy levels have been determined for 28 known lines provides opportunities for calulation by SMSE method to obtain Stark widths and shifts. We analyzed the shift-to-width ratio for all lines and observed the usual deviations as in previous studies of the transition metal group. We determined the influence of Stark broadening mechanism in the Atmosphere of a DA type white dwarf. The Stark broadening mechanism is very important for white dwarfs atmospheres, and one has to take into account this effect for their investigations, analysis and modeling.

Acknowledgements. This work is supported by Ministry of Science, Technological Development and Innovation of the Republic of Serbia through the project contracts No. 451-03-66/2024-03/200002.

Table 1. Electron-impact (Stark) broadening full widths at half intensity maximum (W) and shifts (d) for Hf II spectral lines, for a perturber density of 10^{17} cm^{-3} and temperatures from 5000 K to 80000 K.

Transition	T [K]	W [Å]	d [Å]	W [10^{12} s^{-1}]	d [10^{12} s^{-1}]	$\frac{3kT}{2\Delta E}$
	5000	0.103D+00	-0.223D-01	0.344	-0.074	0.124
Hf II	10000	0.733D-01	-0.158D-01	0.243	-0.052	0.248
$a^4F_{3/2}$ - 6p $y^4D^o_{1/2}$	20000	0.519D-01	-0.111D-01	0.172	-0.037	0.497
2381.03 Å	40000	0.367D-01	-0.791D-02	0.121	-0.026	0.993
	80000	0.259D-01	-0.559D-02	0.086	-0.018	1.986
	5000	0.101D+00	-0.210D-01	0.354	-0.073	0.121
Hf II	10000	0.718D-01	-0.148D-01	0.250	-0.051	0.242
6s $a^4F_{3/2}$ - 6p $y^4D^o_{3/2}$	20000	0.508D-01	-0.105D-01	0.177	-0.036	0.485
2323.98 Å	40000	0.359D-01	-0.744D-02	0.125	-0.025	0.969
	80000	0.254D-01	-0.526D-02	0.088	-0.018	1.939
	5000	0.992D-01	-0.196D-01	0.366	-0.072	0.118
Hf II	10000	0.701D-01	-0.138D-01	0.259	-0.051	0.236
6s $a^4F_{3/2}$ - 6p $y^4D^o_{5/2}$	20000	0.496D-01	-0.979D-02	0.183	-0.036	0.471
2259.39 Å	40000	0.350D-01	-0.692D-02	0.129	-0.025	0.942
	80000	0.248D-01	-0.490D-02	0.091	-0.018	1.885
	5000	0.112D+00	-0.269D-01	0.318	-0.076	0.134
Hf II	10000	0.791D-01	-0.190D-01	0.225	-0.054	0.268
6s $a^4F_{3/2}$ - 6p $y^4F^o_{3/2}$	20000	0.559D-01	-0.134D-01	0.159	-0.038	0.536
2572.45 Å	40000	0.395D-01	-0.953D-02	0.112	-0.027	1.073
	80000	0.279D-01	-0.674D-02	0.079	-0.019	2.146
	5000	0.108D+00	-0.251D-01	0.328	-0.075	0.130
Hf II	10000	0.768D-01	-0.177D-01	0.231	-0.053	0.260
6s $a^4F_{3/2}$ - 6p $y^4F^o_{5/2}$	20000	0.543D-01	-0.125D-01	0.164	-0.037	0.521
2497.75 Å	40000	0.384D-01	-0.889D-02	0.116	-0.026	1.042
	80000	0.271D-01	-0.628D-02	0.082	-0.018	2.084
	5000	0.145D+00	-0.439D-01	0.268	-0.081	0.167
Hf II	10000	0.102D+00	-0.310D-01	0.189	-0.057	0.333
6s $a^4F_{3/2}$ - 6p $z^4G^o_{5/2}$	20000	0.727D-01	-0.219D-01	0.134	-0.040	0.666
3195.12 Å	40000	0.514D-01	-0.155D-01	0.094	-0.028	1.333
	80000	0.363D-01	-0.109D-01	0.067	-0.020	2.665
	5000	0.108D+00	-0.228D-01	0.357	-0.075	0.125
Hf II	10000	0.769D-01	-0.161D-01	0.252	-0.053	0.250
6s $a^4F_{5/2}$ - 6p $y^4D^o_{3/2}$	20000	0.544D-01	-0.114D-01	0.178	-0.037	0.499
2394.09 Å	40000	0.384D-01	-0.808D-02	0.126	-0.026	0.999
	80000	0.272D-01	-0.571D-02	0.089	-0.018	1.997
	5000	0.106D+00	-0.212D-01	0.369	-0.074	0.121
Hf II	10000	0.750D-01	-0.150D-01	0.261	-0.052	0.243
6s $a^4F_{5/2}$ - 6p $y^4D^o_{5/2}$	20000	0.530D-01	-0.106D-01	0.184	-0.037	0.485
2325.61 Å	40000	0.375D-01	-0.751D-02	0.130	-0.026	0.970
	80000	0.265D-01	-0.531D-02	0.092	-0.018	1.940
	5000	0.104D+00	-0.199D-01	0.380	-0.072	0.118
Hf II	10000	0.736D-01	-0.141D-01	0.268	-0.051	0.237
6s $a^4F_{5/2}$ - 6p $y^4D^o_{7/2}$	20000	0.520D-01	-0.999D-02	0.190	-0.036	0.474
2271.39 Å	40000	0.368D-01	-0.706D-02	0.134	-0.025	0.947
	80000	0.260D-01	-0.499D-02	0.095	-0.018	1.895
	5000	0.120D+00	-0.294D-01	0.322	-0.078	0.139
Hf II	10000	0.854D-01	-0.208D-01	0.227	-0.055	0.277
6s $a^4F_{5/2}$ - 6p $y^4F^o_{3/2}$	20000	0.604D-01	-0.147D-01	0.161	-0.039	0.554
2658.64 Å	40000	0.427D-01	-0.104D-01	0.113	-0.027	1.109
	80000	0.302D-01	-0.735D-02	0.080	-0.019	2.218

Table 1. Continued

Transition	T [K]	W [Å]	d [Å]	W [10^{12} s^{-1}]	d [10^{12} s^{-1}]	$\frac{3kT}{2\Delta E}$
	5000	0.117D+00	-0.274D-01	0.331	-0.077	0.134
Hf II	10000	0.827D-01	-0.193D-01	0.234	-0.054	0.269
6s $a^4F_{5/2}$ - 6p $y^4F^o_{5/2}$	20000	0.585D-01	-0.137D-01	0.165	-0.038	0.538
2578.92 Å	40000	0.413D-01	-0.968D-02	0.117	-0.027	1.076
	80000	0.292D-01	-0.684D-02	0.082	-0.019	2.151
	5000	0.114D+00	-0.262D-01	0.337	-0.077	0.132
Hf II	10000	0.811D-01	-0.185D-01	0.238	-0.054	0.264
6s $a^4F_{5/2}$ - 6p $y^4F^o_{7/2}$	20000	0.574D-01	-0.131D-01	0.168	-0.038	0.528
2531.96 Å	40000	0.406D-01	-0.927D-02	0.119	-0.027	1.056
	80000	0.287D-01	-0.655D-02	0.084	-0.019	2.112
	5000	0.159D+00	-0.486D-01	0.271	-0.082	0.174
Hf II	10000	0.113D+00	-0.344D-01	0.192	-0.058	0.347
6s $a^4F_{5/2}$ - 6p $z^4G^o_{5/2}$	20000	0.799D-01	-0.243D-01	0.135	-0.041	0.694
3329.17 Å	40000	0.565D-01	-0.172D-01	0.096	-0.029	1.389
	80000	0.399D-01	-0.121D-01	0.067	-0.020	2.777
	5000	0.107D+00	-0.297D-01	0.293	-0.080	0.155
Hf II	10000	0.762D-01	-0.210D-01	0.207	-0.057	0.310
6s $a^4F_{5/2}$ - 6p $z^4G^o_{7/2}$	20000	0.539D-01	-0.148D-01	0.146	-0.040	0.621
2631.02 Å	40000	0.381D-01	-0.105D-01	0.103	-0.028	1.242
	80000	0.269D-01	-0.743D-02	0.073	-0.020	2.483
	5000	0.114D+00	-0.233D-01	0.373	-0.075	0.125
Hf II	10000	0.812D-01	-0.165D-01	0.264	-0.053	0.251
6s $a^4F_{7/2}$ - 6p $y^4D^o_{5/2}$	20000	0.574D-01	-0.116D-01	0.186	-0.037	0.502
2406.16 Å	40000	0.406D-01	-0.825D-02	0.132	-0.026	1.004
	80000	0.287D-01	-0.583D-02	0.093	-0.019	2.007
	5000	0.112D+00	-0.219D-01	0.384	-0.074	0.122
Hf II	10000	0.795D-01	-0.155D-01	0.271	-0.053	0.245
6s $a^4F_{7/2}$ - 6p $y^4D^o_{7/2}$	20000	0.562D-01	-0.109D-01	0.192	-0.037	0.490
2348.17 Å	40000	0.397D-01	-0.775D-02	0.135	-0.026	0.979
	80000	0.281D-01	-0.548D-02	0.096	-0.018	1.959
	5000	0.127D+00	-0.303D-01	0.335	-0.079	0.140
Hf II	10000	0.903D-01	-0.214D-01	0.237	-0.056	0.279
6s $a^4F_{7/2}$ - 6p $y^4F^o_{5/2}$	20000	0.638D-01	-0.151D-01	0.167	-0.039	0.559
2678.35 Å	40000	0.451D-01	-0.107D-01	0.118	-0.028	1.117
	80000	0.319D-01	-0.757D-02	0.083	-0.019	2.234
	5000	0.933D-01	-0.216D-01	0.341	-0.079	0.137
Hf II	10000	0.660D-01	-0.152D-01	0.241	-0.055	0.274
6s $a^4F_{7/2}$ - 6p $y^4F^o_{7/2}$	20000	0.466D-01	-0.108D-01	0.170	-0.039	0.548
2269.86 Å	40000	0.330D-01	-0.764D-02	0.120	-0.027	1.096
	80000	0.233D-01	-0.540D-02	0.085	-0.019	2.192
	5000	0.119D+00	-0.260D-01	0.356	-0.077	0.131
Hf II	10000	0.845D-01	-0.184D-01	0.252	-0.054	0.262
6s $a^4F_{7/2}$ - 6p $y^4F^o_{9/2}$	20000	0.598D-01	-0.130D-01	0.178	-0.038	0.524
2513.79 Å	40000	0.422D-01	-0.920D-02	0.126	-0.027	1.049
	80000	0.299D-01	-0.651D-02	0.089	-0.019	2.097
	5000	0.179D+00	-0.549D-01	0.275	-0.084	0.182
Hf II	10000	0.126D+00	-0.388D-01	0.195	-0.059	0.365
6s $a^4F_{7/2}$ - 6p $z^4G^o_{5/2}$	20000	0.895D-01	-0.274D-01	0.137	-0.042	0.729
3496.75 Å	40000	0.632D-01	-0.194D-01	0.097	-0.029	1.459
	80000	0.447D-01	-0.137D-01	0.068	-0.021	2.917

Table 1. Continued

Transition	T [K]	W [Å]	d [Å]	W [10^{12} s^{-1}]	d [10^{12} s^{-1}]	$\frac{3kT}{2\Delta E}$
	5000	0.152D+00	-0.425D-01	0.297	-0.082	0.162
Hf II	10000	0.108D+00	-0.301D-01	0.210	-0.058	0.324
6s $a^4F_{7/2}$ - 6p $z^4G^o_{7/2}$	20000	0.763D-01	-0.212D-01	0.148	-0.041	0.649
3110.01 Å	40000	0.539D-01	-0.150D-01	0.105	-0.029	1.297
	80000	0.381D-01	-0.106D-01	0.074	-0.020	2.594
	5000	0.132D+00	-0.329D-01	0.325	-0.080	0.145
Hf II	10000	0.939D-01	-0.232D-01	0.229	-0.056	0.289
6s $a^4F_{7/2}$ - 6p $z^4G^o_{9/2}$	20000	0.664D-01	-0.164D-01	0.162	-0.040	0.579
2774.18 Å	40000	0.469D-01	-0.116D-01	0.114	-0.028	1.157
	80000	0.332D-01	-0.822D-02	0.081	-0.020	2.314
	5000	0.125D+00	-0.2512-01	0.389	-0.077	0.129
Hf II	10000	0.889D-01	-0.177D-01	0.275	-0.055	0.257
6s $a^4F_{9/2}$ - 6p $y^4D^o_{7/2}$	20000	0.628D-01	-0.125D-01	0.195	-0.038	0.514
2464.93 Å	40000	0.444D-01	-0.888D-02	0.137	-0.027	1.028
	80000	0.314D-01	-0.628D-02	0.097	-0.019	2.056
	5000	0.141D+00	-0.335D-01	0.347	-0.081	0.145
Hf II	10000	0.100D+00	-0.236D-01	0.245	-0.057	0.289
6s $a^4F_{9/2}$ - 6p $y^4F^o_{7/2}$	20000	0.709D-01	-0.167D-01	0.173	-0.040	0.579
2774.83 Å	40000	0.501D-01	-0.118D-01	0.122	-0.028	1.157
	80000	0.354D-01	-0.837D-02	0.086	-0.020	2.315
	5000	0.134D+00	-0.299D-01	0.362	-0.080	0.138
Hf II	10000	0.954D-01	-0.212D-01	0.256	-0.056	0.276
6s $a^4F_{9/2}$ - 6p $y^4F^o_{9/2}$	20000	0.674D-01	-0.149D-01	0.181	-0.040	0.552
2648.09 Å	40000	0.477D-01	-0.106D-01	0.128	-0.028	1.105
	80000	0.337D-01	-0.749D-02	0.090	-0.020	2.209
	5000	0.177D+00	-0.501D-01	0.303	-0.085	0.173
Hf II	10000	0.125D+00	-0.354D-01	0.214	-0.060	0.346
6s $a^4F_{9/2}$ - 6p $z^4G^o_{7/2}$	20000	0.886D-01	-0.250D-01	0.151	-0.042	0.692
3318.21 Å	40000	0.626D-01	-0.177D-01	0.107	-0.030	1.384
	80000	0.443D-01	-0.125D-01	0.075	-0.021	2.768
	5000	0.151D+00	-0.382D-01	0.330	-0.083	0.153
Hf II	10000	0.107D+00	-0.270D-01	0.234	-0.059	0.306
6s $a^4F_{9/2}$ - 6p $z^4G^o_{9/2}$	20000	0.758D-01	-0.191D-01	0.165	-0.041	0.613
2938.64 Å	40000	0.536D-01	-0.135D-01	0.117	-0.029	1.226
	80000	0.379D-01	-0.956D-02	0.082	-0.020	2.451
	5000	0.134D+00	-0.298D-01	0.363	-0.080	0.138
Hf II	10000	0.951D-01	-0.210D-01	0.256	-0.056	0.276
6s $a^4F_{9/2}$ - 6p $z^4G^o_{11/2}$	20000	0.673D-01	-0.149D-01	0.181	-0.040	0.551
2642.20 Å	40000	0.475D-01	-0.105D-01	0.128	-0.028	1.102
	80000	0.336D-01	-0.745D-02	0.090	-0.020	2.204

References

Andersen, T., Petersen, P., & Hauge, O., The solar hafnium abundance. 1976, *Solar Physics*, **49**, 211, DOI:10.1007/BF00162445

Den Hartog, E. A., Lawler, J. E., & Roederer, I. U., Improved Atomic Transition Probabilities for UV and Optical Lines of Hf II and Determination of the Hf Abundance in Two Metal-poor Stars. 2021, *ApJS*, **254**, 5, DOI:10.3847/1538-4365/abe861

Dimitrijević, M. S. & Konjević, N., Simple estimates for Stark broadening of ion lines in stellar plasmas. 1987, *Astronomy and Astrophysics*, **172**, 345

Hill, V., Plez, B., Cayrel, R., et al., First stars. I. The extreme r-element rich, iron-poor halo giant CS 31082-001. Implications for the r-process site(s) and radioactive cosmochronology. 2002, *A&A*, **387**, 560, DOI:10.1051/0004-6361:20020434

Ivarsson, S., Andersen, J., Nordström, B., et al., Improved oscillator strengths and wavelengths for Os I and Ir I, and new results on early r-process nucleosynthesis. 2003, *A&A*, **409**, 1141, DOI:10.1051/0004-6361:20031184

Lawler, J. E., den Hartog, E. A., Labby, Z. E., et al., Improved Laboratory Transition Probabilities for Hf II and Hafnium Abundances in the Sun and 10 Metal-poor Stars. 2007, *ApJS*, **169**, 120, DOI:10.1086/510368

Majlinger, Z., Simić, Z., & Dimitrijević, M. S., On the Stark Broadening of Lu III Spectral Lines. 2015, *Journal of Astrophysics and Astronomy*, **36**, 671, DOI:10.1007/s12036-015-9362-9

Majlinger, Z., Simić, Z., & Dimitrijević, M. S., Stark broadening of Zr IV spectral lines in the atmospheres of chemically peculiar stars. 2017, *Monthly Notices of the Royal Astronomical Society*, **470**, 1911, DOI:10.1093/mnras/stx1321

Moore, C. E., Atomic Energy Levels as Derived from the Analysis of Optical Spectra – Molybdenum through Lanthanum and Hafnium through Actinium. 1971, in *Nat. Stand. Ref. Data Ser. 35, Vol. III (Reprint of NBS Circ. 467, Vol. III, 1958)* (U.S.: Nat. Bur. Stand.)

Ralchenko, Y., Fuhr, J. R., Jou, F. C., et al., New Generation of the NIST Atomic Spectroscopic Databases. 2005, in American Institute of Physics Conference Series, Vol. **771**, *Atomic and Molecular Data and their Applications*, ed. T. Kato, D. Kato, & H. Funaba, 276–285

Reader, J., Corliss, C. H., Wiese, W. L., & Martin, G. A. 1980, *Wavelengths and transition probabilities for atoms and atomic ions: Part 1. Wavelengths, part 2. Transition probabilities*

Roederer, I. U., Lawler, J. E., Sobeck, J. S., et al., New Hubble Space Telescope Observations of Heavy Elements in Four Metal-Poor Stars. 2012, *ApJS*, **203**, 27, DOI:10.1088/0067-0049/203/2/27

Russell, H. N., On the Composition of the Sun's Atmosphere. 1929, *ApJ*, **70**, 11, DOI:10.1086/143197

Sahal-Bréchot, S., Impact Theory of the Broadening and Shift of Spectral Lines due to Electrons and Ions in a Plasma. 1969a, *Astronomy and Astrophysics*, **1**, 91

Sahal-Bréchot, S., Impact Theory of the Broadening and Shift of Spectral Lines due to Electrons and Ions in a Plasma (Continued). 1969b, *Astronomy and Astrophysics*, **2**, 322

Sahal-Brechot, S., Dimitrijevic, M., & Nessib, N., Widths and Shifts of Isolated Lines of Neutral and Ionized Atoms Perturbed by Collisions With Electrons and Ions: An Outline of the Semiclassical Perturbation (SCP) Method and of the Approximations Used for the Calculations. 2014, *Atoms*, **2**, 225, DOI:10.3390/atoms2020225

Simić, Z., Milovanović, N., Sakan, N., & Malović, M., On the Stark broadening of the Re II spectral lines. 2023, *Advances in Space Research*, **71**, 1287, DOI:10.1016/j.asr.2022.07.079

Simić, Z. & Sakan, N. M., The electron-impact broadening of the Nb III for 5p-5d transitions. 2020, *Monthly Notices of the Royal Astronomical Society*, **491**, 4382, DOI:10.1093/mnras/stz3362

Simić, Z. & Sakan, N. M., Stark Widths and Shifts of Rh II in Chemically Peculiar Stars. 2021, *International Astronomy and Astrophysics Research Journal*, **3**, 37

Simić, Z., Sakan, N. M., Milovanović, N., & Martinović, M., Singly Ionized Iridium Spectral Lines in the Atmosphere of Hot Stars. 2021, *International Astronomy and Astrophysics Research Journal*, **3**, 33

Sneden, C., Cowan, J. J., Lawler, J. E., et al., The Extremely Metal-poor, Neutron Capture-rich Star CS 22892-052: A Comprehensive Abundance Analysis. 2003, *ApJ*, **591**, 936, DOI:10.1086/375491

Sneden, C., McWilliam, A., Preston, G. W., et al., The Ultra–Metal-poor, Neutron-Capture–rich Giant Star CS 22892-052. 1996, *ApJ*, **467**, 819, DOI:10.1086/177656

Wickramasinghe, D. T., Model atmospheres for DA and DB white dwarfs. 1972, *Memoirs of the Royal Astronomical Society*, **76**, 129

Yushchenko, A., Gopka, V., Goriely, S., et al., Thorium-rich halo star HD 221170: Further evidence against the universality of the r-process. 2005, *A&A*, **430**, 255, DOI:10.1051/0004-6361:20041540